

Profiling of formaldehyde, glyoxal, methylglyoxal, and CO over the Amazon: Normalised excess mixing ratios and related emission factors in biomass burning plumes

Interactive comment, editor review

Editor review: The reply to the first reviewer comment RC1 is lacking quantitative information. Please clarify how significant is the impact of fitting/not fitting water vapour absorption in the glyoxal retrieval scheme. E.g. give an estimate of the typical percent change of the dSCD when including/excluding H₂O, for cases where the signal is strong enough. The reason why H₂O misfits are problematic for glyoxal but not for methylglyoxal also remains a bit obscure.

Our responses:

Glyoxal: For a better comparison of the glyoxal retrieval including/excluding the water absorption at 442 nm (the 7v water vapour band), we analysed the DOAS retrieval using a fitting window ranging from 425 to 439 nm and simultaneously at 447 to 465 nm (as described in the manuscript) as well as a continuous spectral range from 425 to 465 nm. An example retrieval using the continuous spectral range of the same skylight spectrum as shown in the manuscript (fig. 1, panel 2) is attached to this response (fig. 1), and a scatter plot of the dSCD's of both retrievals is shown in fig. 2.

For altitudes below 2 km flight altitude, where the water vapour and glyoxal absorption are the strongest, the dSCD's obtained from the continuous fit window are typically 12% smaller than those discarding the 7v water vapour absorption band. This is presumably because part of the glyoxal absorption structure between 425 to 430 nm is removed by the not well represented weak water vapour band located between the 7v+ δ and 7v bands (c.f., see Lampel et al., Atmos. Meas. Tech., 8, 4329–4346, <https://doi.org/10.5194/amt-8-4329-2015>, 2015). For larger altitudes and with decreasing water vapour and glyoxal absorption, the difference may even become larger and more variable with a mean percentage change as large as 80%. The dSCD's inferred from the continuous fitting window typically remain smaller than those discarding the 7v water vapour band as shown in the attached fig. 2.

Methylglyoxal and higher carbonyls, briefly called methylglyoxal*: The mean difference including/excluding the 7v water vapour band is in the order of 75% for observations below 2 km and up to 145% below 6 km flight altitude, with the smaller methylglyoxal* dSCD's obtained from the continuous fitting range. An example retrieval using the fitting range excluding the water band at 442 nm is attached (fig. 3) using the same skylight spectrum as shown in fig. 1, panel 3 in the manuscript for the continuous fit range.

As for the glyoxal retrieval, the relative difference among both retrievals increases with the flight altitude, i.e. with smaller methylglyoxal* and water vapour absorption (a scatter plot corresponding to figure 2 is attached (fig. 4)). At this point, the potential causes for the interference of the 7v water vapour band and methylglyoxal* absorption bands in the retrieval are subject to further investigation. From the spectral retrieval, we conclude that when discarding the 7v water band, the 6v+ δ band becomes the relevant absorption band for the retrieval of water vapour, while any remaining spectral structure around the 7v water vapour is attributed to the absorption of methylglyoxal and 2,3-butanedione (and higher carbonyls). As a result, the amplitudes for methylglyoxal and 2,3-butanedione are increasing by the given amounts (i.e. on average by 75% below 2 km and on average by 145% below 6 km), while the overall spectral residuals are decreasing. Based on fig. 4 and our flight analysis, this effect seems to be enhanced at lower flight altitudes and when passing biomass burning plumes. The latter clearly demonstrates the presence of elevated amounts of methylglyoxal and 2,3-butanedione (and higher carbonyls) in the biomass burning plumes.

However, as described in the manuscript, the spectral resolution of the spectrometers does not allow for a more selective spectral retrieval of methylglyoxal, 2,3-butanedione, and higher carbonyls, and thus we are left to decide as to whether the inclusion/exclusion of the 7v water band is more appropriate. Mainly based on the reduced residual structure, we decided to include the 7v water vapour band in the retrieval in a similar way as Zarzana et al., (2018). We note however, that the stated uncertainty of the methylglyoxal* retrieval (a factor of 2 for altitudes <2 km and somewhat larger for altitudes <6 km) is larger than the mean difference of 75% or 145%, respectively, between both retrieval settings, and thus the uncertainties arising from the above mentioned interference are covered by our uncertainty estimate.

Attached figures:

Figure 1: Inferred absorption spectrum and residual structure of glyoxal for the measurement at 15:06 UTC during the flight on Sept. 11, 2014 (AC11) according to fig. 1, panel 2 in the manuscript. The continuous fit range from 420 - 465 nm includes the 7v water vapour band.

Figure 2: Differential slant column densities of glyoxal based on a spectral retrieval excluding the 7v water vapour band (x-axis) and including it (y-axis) from measurement flights AC09, AC11, AC12, and AC13. The colour coding shows the respective flight altitudes.

Figure 3: Inferred absorption spectrum and residual structure of methylglyoxal* for the measurement at 14:53 UTC during the flight on Sept. 11, 2014 (AC11) according to fig. 1, panel 3 in the manuscript. The discrete fit range from 420 – 439 and 447 – 475 nm includes the 7v water vapour band.

Figure 4: Differential slant column densities of methylglyoxal* based on a spectral retrieval excluding the 7v water vapour band (x-axis) and including it (y-axis) from measurement flights AC09, AC11, AC12, and AC13. The colour coding shows the respective flight altitudes.

No changes to the manuscript Version 3 from July 14th have been made.

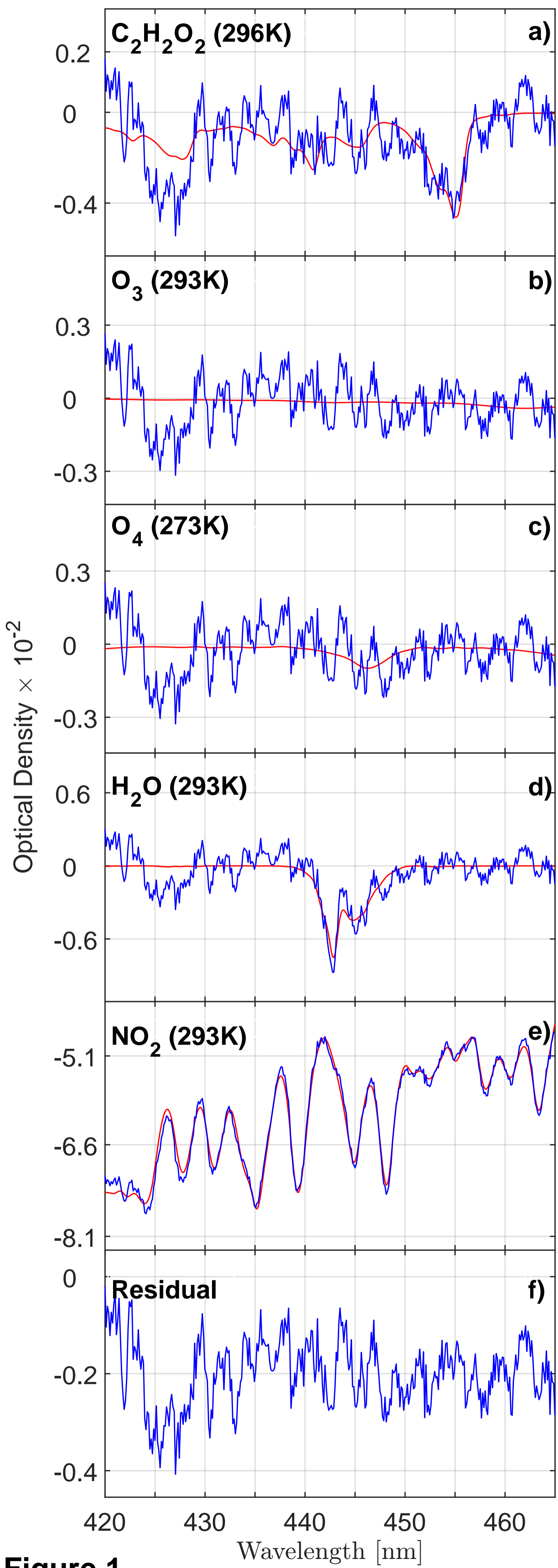


Figure 1

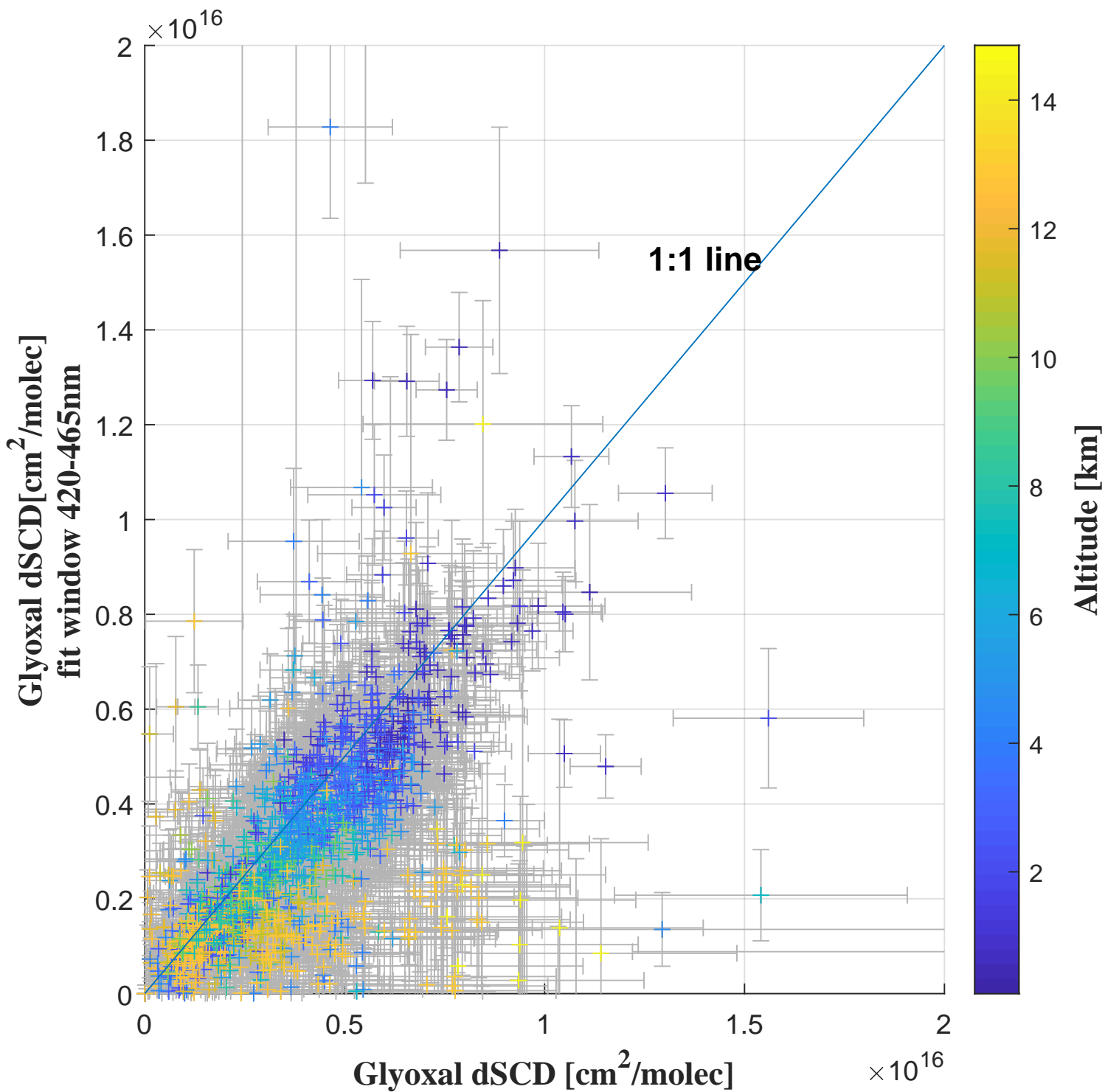


Figure 2

fit window 420-439nm and 447-465nm

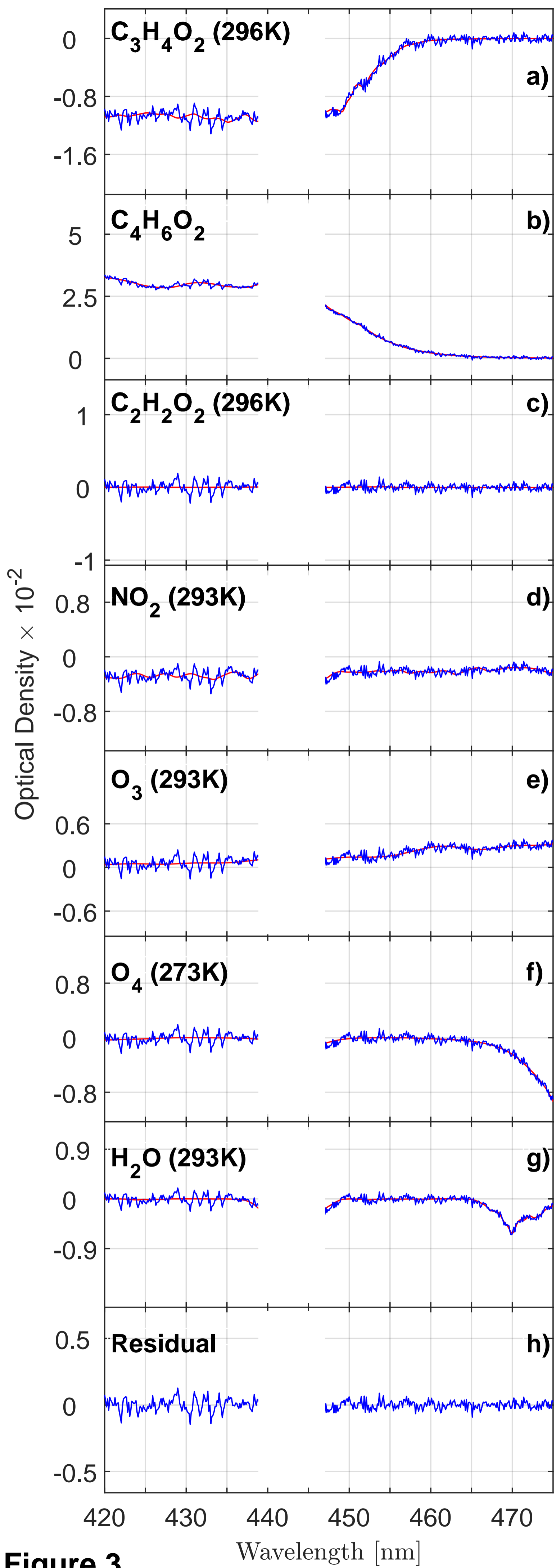


Figure 3

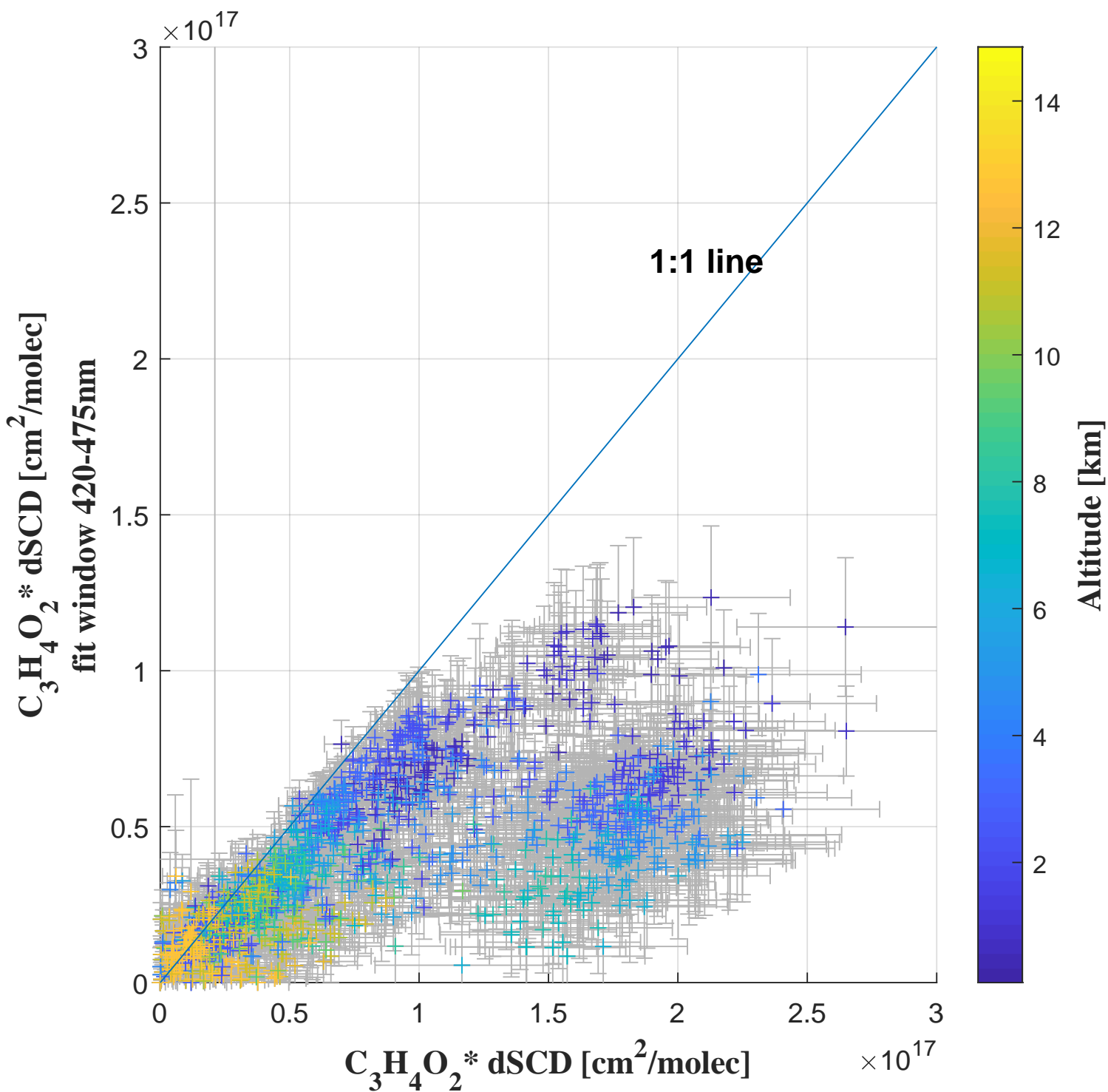


Figure 4

fit window 420-439nm and 447-475nm